Central Role of Manganese in Regulation of Stress Responses, Physiology, and Metabolism in *Streptococcus pneumoniae*[▽][†]

Abiodun D. Ogunniyi,[1] Layla K. Mahdi,[1] Michael P. Jennings,[2] Alastair G. McEwan,[3] Christopher A. McDevitt,[1] Mark B. Van der Hoek,[4] Christopher J. Bagley,[5] Peter Hoffmann,[5] Katherine A. Gould,[6] and James C. Paton[1]*

Research Centre for Infectious Diseases, School of Molecular and Biomedical Science, The University of Adelaide, Adelaide, SA 5005, Australia[1]; Institute for Glycomics, Griffith University, Gold Coast Campus, Queensland, 4222, Australia[2]; School of Chemistry and Molecular Biosciences, University of Queensland, Brisbane, Queensland, 4072, Australia[3]; Adelaide Microarray Centre, The University of Adelaide and Hanson Institute, Adelaide, SA 5000, Australia[4]; Adelaide Proteomics Centre, School of Molecular and Biomedical Science, The University of Adelaide, Adelaide, SA 5005, Australia[5]; and Bacterial Microarray Group, St. George's, University of London, London SW17 0RE, United Kingdom[6]

The importance of Mn^{2+} for pneumococcal physiology and virulence has been studied extensively. However, the specific cellular role(s) for which Mn^{2+} is required are yet to be fully elucidated. Here, we analyzed the effect of Mn^{2+} limitation on the transcriptome and proteome of *Streptococcus pneumoniae* D39. This was carried out by comparing a deletion mutant lacking the solute binding protein of the high-affinity Mn^{2+} transporter, pneumococcal surface antigen A (PsaA), with its isogenic wild-type counterpart. We provide clear evidence for the Mn^{2+}-dependent regulation of the expression of oxidative-stress-response enzymes SpxB and Mn^{2+}-SodA and virulence-associated genes *pcpA* and *prtA*. We also demonstrate the upregulation of at least one oxidative- and nitrosative-stress-response gene cluster, comprising *adhC*, *nmlR*, and *czcD*, in response to Mn^{2+} stress. A significant increase in 6-phosphogluconate dehydrogenase activity in the *psaA* mutant grown under Mn^{2+}-replete conditions and upregulation of an oligopeptide ABC permease (AppDCBA) were also observed. Together, the results of transcriptomic and proteomic analyses provided evidence for Mn^{2+} having a central role in activating or stimulating enzymes involved in central carbon and general metabolism. Our results also highlight the importance of high-affinity Mn^{2+} transport by PsaA in pneumococcal competence, physiology, and metabolism and elucidate mechanisms underlying the response to Mn^{2+} stress.

Divalent cations are essential micronutrients for the growth and survival of bacteria in diverse environmental niches, including sites within higher organisms. One strategy employed by host organisms is to limit bacterial growth by restricting metal ion availability by sequestration with high-affinity metal binding proteins (7). To overcome these innate defenses, bacteria have evolved both metal ion-chelating mechanisms and high-affinity transport systems, enabling them to scavenge essential metals *in vivo*. Although the best-studied systems are involved in the acquisition of Fe^{3+}, Mn^{2+} is increasingly being recognized as a critical micronutrient, particularly for pathogenic bacteria. Pneumococcal surface antigen A (PsaA) (47), the Mn^{2+}-specific solute binding component of an ATP-binding cassette (ABC) cation permease encoded by the *psaBCA* locus, is an important virulence factor for *Streptococcus pneumoniae* (43). Mutation of *psaA* has been shown to result in massively reduced virulence in systemic, respiratory tract, and otitis media murine models of infection (4, 33, 34).

PsaA belongs to the cluster IX family of bacterial transporters of the essential metal ions Mn^{2+}, Zn^{2+}, and Fe^{2+} (9). All of the available physiological evidence indicates that it is involved in the transport of Mn^{2+}; the optimal growth and competence for genetic transformation of a *psaA* mutant showed an absolute requirement for additional Mn^{2+} (9, 33, 34). The deletion of *psaB* and *psaC*, which encode the transmembrane and ATP-binding components of the Psa permease, also results in a requirement for Mn^{2+} (33, 34, 37). Despite this physiological evidence, the high-resolution structure of PsaA showed a Zn^{2+} ion occupying the metal binding site (29). However, Zn^{2+} transport seems unlikely to be the primary physiological function for PsaBCA for two reasons; first, two specific ABC cassette transporters for Zn^{2+} (AdcRCBA and AdcAII) are present in *S. pneumoniae*, and second, Zn^{2+} negatively regulates PsaBCA expression via PsaR (9, 32).

There is a large body of evidence that PsaA plays a role in resistance to oxidative stress (18, 19, 34, 57). The most obvious explanation for this observation is the presence of the Mn^{2+}-dependent superoxide dismutase Mn^{2+} SodA, which protects the cell from superoxide, in the pneumococcus. The observation that *psaA* mutants exhibit a 40% reduction in Sod activity in the absence of Mn^{2+} is consistent with this interpretation (57, 58). Interestingly, one microarray study identified a two-component system that controls the expression of PsaA and regulates virulence and resistance to oxidative stress, albeit in a serotype-specific manner (35).

The above-described studies indicate that Mn^{2+} is associated with a diverse range of cellular metabolic and regulatory processes. However, the presence of high-affinity Mn^{2+} trans-

porters has prevented the manipulation of intracellular Mn^{2+} levels in wild-type bacteria to allow elucidation of these processes. Nevertheless, the intracellular Mn^{2+} concentration can be manipulated in Mn^{2+} transport mutants (9, 34). Thus, in the present study, a combination of transcriptomic and proteomic comparisons of wild-type and *psaA* mutant *S. pneumoniae* under Mn^{2+}-replete and Mn^{2+}-limiting conditions has enabled the first systematic investigation of the role of Mn^{2+} in the regulation of metabolism and stress response physiology in *S. pneumoniae*.

FIG. 1. Western blot analysis of PsaA expression in *S. pneumoniae* D39 and its isogenic *psaA* deletion mutant lysates. Bacteria were grown in C+Y+M (with 3 μM added $MnSO_4$) or C+Y (without added $MnSO_4$) medium. D+, D39 wild type grown in C+Y+M medium; D−, D39 wild type grown in C+Y medium; A+, D39 *psaA* deletion mutant grown in C+Y+M medium; A−, D39 *psaA* deletion mutant grown in C+Y medium.

MATERIALS AND METHODS

Bacterial strains and growth conditions. The *S. pneumoniae* strains used in this study are D39 (3) and its isogenic unmarked, in-frame *psaA* deletion mutant (34). Frozen stocks of the two strains were prepared by growing them at 37°C to an A_{600} of 0.4 in a semisynthetic casein hydrolysate medium supplemented with 0.5% yeast extract without added $MnSO_4$ (C+Y medium) (27), as described previously (34). The cultures were concentrated 20× in C+Y medium, glycerol was added to a final concentration of 15%, and then the cultures were stored at −80°C. For *in vitro* growth measurements and proteomic and transcriptomic analyses, cultures from frozen stocks were added to C+Y medium or to C+Y medium with 3 μM $MnSO_4$ (C+Y+M medium). Cultures were incubated at 37°C, and growth measured at regular intervals until an A_{600} of 0.5 was reached. The experiment was performed four times, and for each growth condition, cells were harvested and processed for either transcriptomic or proteomic analysis.

Microarray protocol and data analysis. RNA was extracted from bacterial pellets with acid-phenol/chloroform/isoamyl alcohol (125:24:1 [pH 4.5]; Ambion) and checked for purity and integrity as described previously (30, 38). Microarray experiments were performed on whole-genome *S. pneumoniae* PCR arrays based on TIGR4 and R6 annotations (55). Array slides were obtained from the Bacterial Microarray Group at St. George's, University of London. The array design is available in BμG@Sbase (accession no. A-BUGS-14; http://bugs.sgul.ac.uk/A-BUGS-14) and, also, ArrayExpress (accession no. A-BUGS-14).

Fluorescently labeled cDNAs were hybridized to the surface of the microarray as described previously (35). The Spot plug-in (CSIRO, Australia) within the R statistical software package (http://www.R-project.org) and the Limma plug-in for R (49) were used for data processing and statistical analysis. The ratio values were normalized using the print-tip Loess normalization routine (51), and a linear model fitted to determine a final expression value for each mRNA (50). These statistics were used to rank the mRNAs from those most likely to be differentially expressed to the least likely using a false discovery rate of a *P* value of <0.05. Details of protocol and analysis are in the supplemental material. Fully annotated microarray data have been deposited in BμG@Sbase (accession no. E-BUGS-89; http://bugs.sgul.ac.uk/E-BUGS-89) and, also, ArrayExpress (accession no. E-BUGS-89).

2D DIGE and data analysis. Proteins were extracted using a modification of the method described previously (12). Proteins were labeled with Cy2, Cy3, or Cy5 CyDye DIGE fluors (GE Healthcare) and subjected to two-dimensional (2D) difference gel electrophoresis (DIGE) according to the manufacturer's protocol. After electrophoresis, gels were scanned for fluorescence using an Ettan DIGE imager (GE Healthcare). Image analysis was undertaken using the Differential In-gel Analysis (DIA) module in DeCyder 2D software (version 6.5; GE Healthcare). Protein spots chosen for identification were picked robotically (Ettan SpotCutter; GE Healthcare) from two gels using pick coordinates assigned by DeCyder software. Principal components analysis (PCA) and hierarchical clustering analysis (HCA) were conducted according to the DeCyder Extended Data Analysis user manual, version 7.0. If more than one protein was identified in each spot, the relative abundance of each protein was determined from the emPAI (exponentially modified protein abundance index) score reported by MASCOT and the assumption made that the most abundant protein would account for the observed regulation (see the supplemental material). In some instances, the relative abundances of identified proteins in pair-wise comparisons were further validated by reverse transcription (RT)-PCR. Secondary identification of the protein spots was also carried out on preparative silver-stained gels. Further details of these procedures and statistical analyses are in the supplemental material.

Real-time RT-PCR. For a subset of selected genes, differences in the levels of expression obtained by transcriptomic and proteomic analysis were validated by one-step relative quantitative real-time RT-PCR in a Roche LC480 real-time cycler, essentially as described previously (46). The specific primers used for the various RT-PCR assays are listed in Table S1 in the supplemental material and

were used at a final concentration of 200 nM per reaction. As an internal control, primers specific for the 16S rRNA were employed. The amplification data were analyzed using the comparative critical threshold ($2^{-\Delta\Delta CT}$) method (31).

6-PGD enzymatic activity assay. An enzymatic activity assay for (6-phosphogluconate dehydrogenase) 6-PGD was carried out as described previously (5) and as detailed in the supplemental material.

SDS-PAGE and Western blotting. Bacteria were lysed in lysis buffer and subjected to SDS-PAGE as described previously (28). Separated proteins were electroblotted onto nitrocellulose (Pall Life Sciences, MI) as described previously (56). After transfer, the membrane was probed with specific polyclonal mouse anti-PsaA serum at a dilution of 1/3,000 and then reacted with blotting-grade goat anti-mouse alkaline phosphatase conjugate (Bio-Rad Laboratories, Hercules, CA).

Metal content determination. Metal content determination was performed by inductively coupled plasma mass spectrometry (ICPMS) using wild-type and mutant cells grown to an A_{600} of 0.3 in either C+Y or C+Y+M medium on an Agilent 7500cx ICPMS essentially as described previously (34).

RESULTS

Transcriptome and proteome analyses of wild-type *S. pneumoniae* D39 and its isogenic unmarked, in-frame *psaA* deletion mutant. This study used a systematic approach integrating transcriptomic (microarray) and proteomic (two-dimensional [2D] difference gel electrophoresis [DIGE]) comparisons of wild-type *S. pneumoniae* D39 (D) and an otherwise isogenic unmarked, in-frame *psaA* deletion mutant thereof (A). Each of these was grown under Mn^{2+}-replete (+) and Mn^{2+}-limiting (−) conditions (C+Y medium with or without 3 μM $MnSO_4$, respectively). To confirm that the selected conditions were appropriate for the investigation of Mn^{2+}-dependent responses, we investigated PsaA expression by Western blot analysis of whole-cell lysates using mouse polyclonal anti-PsaA serum. As expected (18), the expression of PsaA in wild-type cells grown in Mn^{2+}-limiting conditions (D−) was markedly higher than its expression in cells grown in Mn^{2+}-replete medium (D+), with no product observed for the mutant strain in either medium (A− or A+) (Fig. 1).

The effect of Mn^{2+} limitation on gene expression in wild-type cells. The effect of Mn^{2+} limitation on gene expression in wild-type (D− versus D+) cells was then investigated, and based on the results of previous studies (18, 23), it was expected that genes under the control of the Mn^{2+}-responsive transcription factor PsaR would show altered levels of expression. The results in Table 1 and, also, in Table S5 in the supplemental material show that, in the absence of Mn^{2+}, there was a significant increase in the relative transcript levels of *psaB*, *psaC*, and *psaA*, consistent with derepression of the *psa* operon as a consequence of Mn^{2+} limitation. Other pneumococcal virulence-associated genes, such as *pcpA* (spd1965) and *prtA* (spd0558), also showed large increases in relative transcript levels in response to Mn^{2+} limitation, and it is known that these genes are also part of the PsaR regulon (16,

TABLE 1. Microarray analysis of *S. pneumoniae* D39 wild type and its isogenic *psaA* deletion mutant counterpart grown in C+Y medium with and without 3 μM added Mn^{2+}

Gene ID[a]		Gene annotation	Fold change[b]				
Strain R6 or TIGR4	Strain D39		A− vs A+	A+ vs D−	A+ vs D+	A− vs D−	D− vs D+
0014	0014	Transcriptional regulator ComX1	N.S.	N.S.	N.S.	−8.4	N.S.
0641	0558	Serine protease, subtilase family (PrtA)	16.1	−13.7	N.S.	N.S.	21.69
0766	0667	SodA; superoxide dismutase, manganese-dependent	−2.1	N.S.	N.S.	N.S.	N.S.
SpR6-1191	1167	AppD; ABC transporter ATP-binding protein	N.S.	2.7	2.7	N.S.	N.S.
SpR6-1193	1169	AppB; ABC transporter membrane-spanning permease	N.S.	3.0	2.7	N.S.	N.S.
SpR6-1194	1170	AppA; ABC transporter substrate-binding protein (oligopeptide transport)	N.S.	2.3	2.4	N.S.	N.S.
1648	1461	Manganese ABC transporter, ATP-binding protein (PsaB)	6.7	−7.6	N.S.	N.S.	8.51
1649	1462	Manganese ABC transporter, permease protein (PsaC)	7.6	−7.4	N.S.	N.S.	12.68
1855	1636	Alcohol dehydrogenase, zinc containing (AdhC)	3.9	N.S.	N.S.	3.5	N.S.
1856	1637	Transcriptional regulator, MerR family protein (NmlR)	4.7	N.S.	N.S.	3.1	N.S.
1857	1638	Cation efflux system protein (CzcD)	7.8	−3.4	N.S.	N.S.	4.60
2136	1965	Choline binding protein PcpA	27.3	−8.7	N.S.	3.1	12.99

[a] Gene sequences were obtained from the *S. pneumoniae* R6, D39, or TIGR4 genome as deposited in the Kyoto Encyclopedia of Genes and Genomes (KEGG) database.

[b] A+, D39 *psaA* deletion mutant grown in C+Y medium with 3 μM added Mn^{2+}; A−, D39 *psaA* deletion mutant grown in C+Y medium without added Mn^{2+}; D+, D39 wild type grown in C+Y medium with 3 μM added Mn^{2+}; D−, D39 wild type grown in C+Y medium without added Mn^{2+}. Values are for the first indicated phenotype; N.S. indicates that the comparison did not yield a value reaching statistical significance.

18, 23). The *czcD* gene, which encodes a zinc efflux pump, also showed increased mRNA levels in response to Mn^{2+} limitation (Table 1); in contrast to the other genes described above, *czcD* expression is activated by the Zn^{2+}-responsive transcription factor SczA (22, 53) rather than PsaR.

The effect of Mn^{2+} limitation on gene expression in the *psaA* mutant. The effect of Mn^{2+} limitation on gene expression in the *psaA* mutant (A− versus A+) was also investigated. The five genes that showed increased relative transcript levels in response to Mn^{2+} limitation in wild-type cells also showed an increase in the mutant strain. However, there were three additional changes; genes encoding the MerR family transcription factor (NmlR) and a glutathione (GSH)-dependent alcohol dehydrogenase (AdhC) also showed increased expression, while *sodA* (encoding Mn^{2+}-dependent superoxide dismutase [SOD]) showed a small decrease in its relative transcript amount (Table 1; also see Tables S2A, C, and D in the supplemental material). It is notable that *czcD*, *nmlR*, and *adhC* form a gene cluster (spd1636 to spd1638 [spd1636-1638]) whose transcription is coupled under some conditions (22, 53).

Effect of mutation of *psaA* on gene expression. Our observation that the *psaA* mutant grown under conditions of Mn^{2+} supplementation (A+) had a cellular concentration of Mn^{2+} comparable to that in wild-type cells grown under conditions of Mn^{2+} limitation (D−) enabled us to determine whether the loss of PsaA alone had an effect on gene expression. The results in Table 1 show that the relative transcript levels of genes under PsaR control were much lower in the *psaA* mutant than in wild-type cells even though the cellular Mn^{2+} concentration in both strains was similar. Similarly, the *czcD* gene exhibited a lower transcript level in the *psaA* mutant than in the wild-type strain. A gene cluster encoding an ABC cassette transport protein, predicted to encode an oligopeptide permease, was also observed to increase its relative transcript amount in the A+ cells compared to its transcript amounts in D− and D+ cells. Taken together, these data suggest that the absence of the PsaA protein might be linked to a change in gene expression that was independent of the cellular Mn^{2+} concentration.

Effect of Mn^{2+} limitation on growth. The requirement for Mn^{2+} supplementation for the growth of *psaA* mutants was investigated. As expected (9, 19, 34), mutant bacteria grown without added Mn^{2+} (A−) had an extended lag phase, whereas mutant bacteria grown in the presence of 3 μM MnSO$_4$ (A+) had an almost wild-type growth rate (see Fig. S1 in the supplemental material).

Proteome analysis. The optimized DIGE and DeCyder analyses of four replicate samples (see the supplemental material) from each of the D+, D−, A+, and A− cells resolved more than 2,000 spots, 61 of which were differentially expressed. The set of spots that showed significant regulation in at least one pair-wise comparison were subjected to PCA using the DeCyder Extended Data Analysis module (version 6.5) (13). This reduction of the dimensionality of the data showed that there was good reproducibility of the spot maps from each experimental group. The spot maps from the four conditions showed that D+ and D− samples clustered together, while A+ and A− samples clustered separately and distant from each other (Fig. 2), indicating that the Mn^{2+}-limiting condition had little overall effect on protein expression in wild-type bacteria. The results of the hierarchical clustering analysis (11) performed subsequently correlated with the PCA results (Fig. 3), confirming the robustness of the strain- and growth medium-dependent protein expression patterns. Of this set of spots, 12 spots that satisfied the selection criteria as defined by the emPAI score reported by MASCOT (see Fig. S2 and Table S6 in the supplemental material) were chosen for identification and differential expression analysis (Table 2 and Fig. 4). Three-dimensional images of standardized log abundances of the Mn^{2+}-dependent superoxide dismutase (SodA; spd0667) and lactate oxidase (LctO; spd0621) are illustrated as examples (Fig. 4).

Analysis of the changes to the proteome of strains grown under the conditions described above revealed some changes
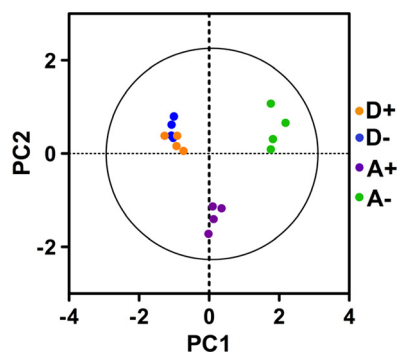
FIG. 2. Principal component analysis of *S. pneumoniae* D39 and its isogenic *psaA* deletion mutant protein spots. Sixty-one differentially expressed protein spots were analyzed. PC1 is the single principal component that accounts for as much of the variability in the data as possible. PC2 is the succeeding uncorrelated (orthogonal) component that accounts for as much of the remaining variability as possible. D+, D39 wild type grown in C+Y+M medium; D−, D39 wild type grown in C+Y medium; A+, D39 *psaA* deletion mutant grown in C+Y+M medium; A−, D39 *psaA* deletion mutant grown in C+Y medium.

in relative protein amounts that were distinct from those observed in the microarray analysis (Table 2). In concordance with the results of PCA and HCA described above, no significant changes in protein levels were observed in the comparison of D− and D+ cells, confirming that, in wild-type bacteria, the Mn^{2+}-limiting condition had a minimal effect on relative protein expression. Under conditions where the cellular concentration of Mn^{2+} was similar (A+ versus D−) a number of changes in relative protein abundance were observed. Five proteins showed a >2-fold increase in abundance in the A+ strain. These proteins included glyceraldehyde 3-phosphate

dehydrogenase (GAPDH), LctO, and elongation factor Tu (EF-Tu)/PepC. Two proteins showed >2-fold lower abundance in A+ cells than in D− cells. These proteins were pyruvate oxidase (SpxB) and PepA, a glutamyl aminopeptidase. The effect of Mn^{2+} on the proteome of a *psaA* mutant was in many cases opposite to those changes observed in the A+/D− comparison. The most notable changes were an increase in the protein abundance of SpxB in the A− strain accompanied by a decrease in LctO and a decrease in SodA. Wherever possible, relative protein amounts were correlated with the corresponding relative mRNA levels.

Metal content determination. ICPMS analysis of wild-type and mutant cells grown to an A_{600} of 0.3 either in C+Y or C+Y+M medium showed that A+ cells had a Mn^{2+} concentration similar to that in wild-type cells grown under conditions of Mn^{2+} limitation (Table 3). The ICPMS data also showed that the PsaA mutants had essentially half the Zn^{2+} concentration of wild-type cells. The Zn^{2+} content data are consistent with transcriptional regulation of *prtA*, *psaBC*, *pcpA*, and *czcD* by the Zn^{2+}-responsive regulator PsaR.

6-PGD enzymatic activity assay. Secondary analysis of proteomic data on preparative silver-stained gels identified 6-phosphogluconate dehydrogenase (6-PGD) (*gnd*; spd0343) as a spot neighboring/overlapping EF-Tu/PepC which the original DIGE experiment was not sensitive enough to identify. Because this enzyme could potentially be activated by Mn^{2+} but has yet to be characterized, we investigated its activity in A+, A−, D+, and D− cells. Two independent experiments were performed; the assays showed 6-PGD activity in cell extracts of A+ and A− cells, with approximately 4.5-fold greater activity in A+ bacteria. However, no detectable activity was observed in the D+ or D− cell extracts.
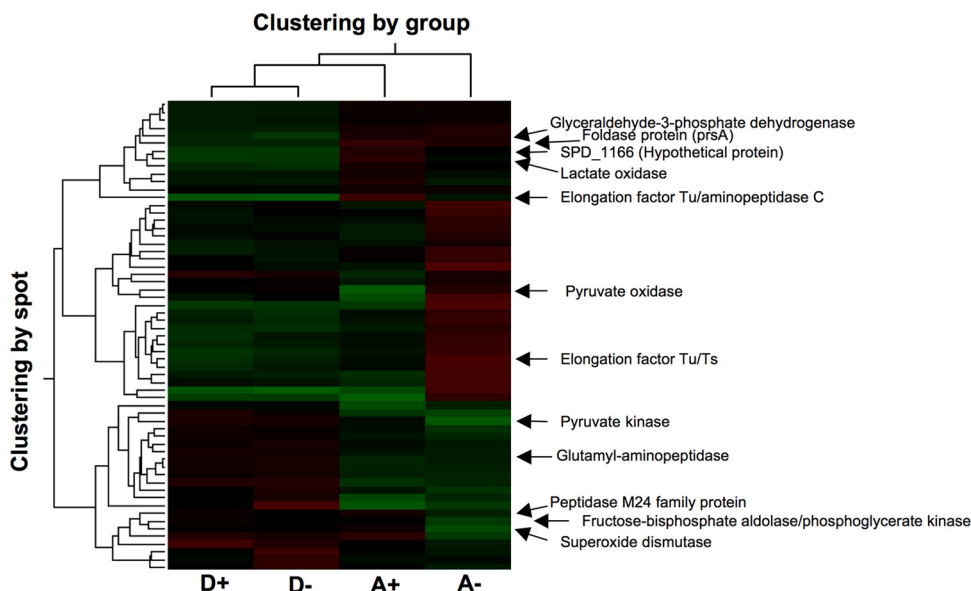
FIG. 3. Hierarchical clustering analysis of *S. pneumoniae* D39 and its isogenic *psaA* deletion mutant protein spots. The wild type and its isogenic *psaA* deletion mutant were grown in C+Y+M or C+Y medium. The relative positions of 12 highly regulated protein spots from the 61 differentially expressed spots are indicated. D+, D39 wild type grown in C+Y+M medium; D−, D39 wild type grown in C+Y medium; A+, D39 *psaA* deletion mutant grown in C+Y+M medium; A−, D39 *psaA* deletion mutant grown in C+Y medium; red, upregulation; green, downregulation.

TABLE 2. DIGE analysis of *S. pneumoniae* D39 wild type and its isogenic *psaA* deletion mutant counterpart grown in C+Y medium with and without 3 μM added Mn²⁺

Locus tag (strain D39)	Protein ID (NCBI GI no.)	Relative abundance (P value)[a]				
		A− vs A+	A+ vs D−	A+ vs D+	A− vs D−	D− vs D+
spd0636	Pyruvate oxidase (116516119)	4.76 (0.1)[b]	−2.65	−1.94	1.80	1.37
spd1166	Hypothetical protein (116515829)	−1.71	3.50 (0.003)	3.35 (0.004)	2.05 (0.014)	−1.04
spd1318/spd0261/ spd0343	Elongation factor Tu (116515356)/aminopeptidase C (116516913)/6-phosphogluconate dehydrogenase	−2.95 (0.002)	5.79 (0.0001)	5.31 (0.001)	1.96	−1.09
spd1318/spd2041	Elongation factor Tu/Ts (116515356/116516076)	3.42 (0.048)	1.12	1.44	3.83 (0.04)	1.29
spd0177	Peptidase M24 family protein (116516135)	−2.03 (0.0001)	1.27	1.11	−1.60	−1.14
spd0868/spd1318	Foldase protein (PrsA) (116517083)/elongation factor Tu (116515356)	−1.23	2.57 (0.003)	2.91 (0.0001)	2.29 (0.004)	1.03
spd1823	Glyceraldehyde-3-phosphate dehydrogenase (116516442)	1.05	2.81 (0.001)	2.22 (0.0001)	2.70 (0.002)	−1.16
spd0526/spd0445	Fructose-biphosphate aldolase (116515860)/phosphoglycerate kinase (116516585)	−2.08 (0.001)	1.12	−1.15	−1.85	−1.29
spd0621	Lactate oxidase (116517149)	−2.06 (0.003)	3.32 (0.001)	3.31 (0.005)	1.61	−1.0
spd0790	Pyruvate kinase (116516870)	−1.80	−1.81 (0.04)	−1.91	−3.26 (0.010)	−1.06
spd0667	Mn²⁺-dependent superoxide dismutase (116515547)	−2.89 (0.0001)	1.30	1.15	−2.21 (0.002)	−1.13
spd1647	Glutamyl aminopeptidase PepA (116516201)	1.18	−2.39 (0.005)	−2.25 (0.015)	−2.03 (0.014)	1.06

[a] A+, D39 *psaA* deletion mutant grown in C+Y medium with 3 μM added Mn²⁺; A−, D39 *psaA* deletion mutant grown in C+Y medium without added Mn²⁺; D+, D39 wild type grown in C+Y medium with 3 μM added Mn²⁺; D−, D39 wild type grown in C+Y medium without added Mn²⁺. Scores without a P value did not reach statistical significance by t test (two-tailed).

[b] This did not meet the t test criteria but was selected on the basis of its high Mn²⁺ dependence in the mutant.

DISCUSSION

The importance of Mn²⁺ for pneumococcal physiology and virulence has been studied extensively. However, the specific cellular role(s) for which Mn²⁺ is required are yet to be fully clarified. In this investigation, we have carried out an extensive analysis of the global effects of Mn²⁺ on the transcriptome and proteome of *S. pneumoniae* D39 by comparing a deletion mutant lacking the solute binding protein of the high-affinity Mn²⁺ transporter, PsaA, with its isogenic wild-type counterpart. Our analysis showed differences between the microarray and proteomic data, and this would not be totally unexpected. This is because while the microarray provides a comprehensive snapshot of transcripts whose levels are altered, proteomic analysis does not provide a similar overview. Some proteins may be not identified by DIGE because of solubility issues, neighboring/overlapping spots, posttranslational modification, and pIs outside the range of the analysis. In the DIGE analysis, there were about 2,000 resolvable spots representing probably only the 1,000 most abundant proteins, taking into account protein isoforms, and we analyzed only 12 of these. Nevertheless, the protein spots identified were further validated by RT-PCR.

The results of the comparison between Mn²⁺-limited (D−) and Mn²⁺-replete (D+) wild-type cells highlight the central role of Mn²⁺ in the regulation of gene expression in the pneumococcus. Genes such as *prtA*, *psaBCA*, and *pcpA* are known to be regulated by the Mn²⁺-dependent repressor PsaR (16, 18, 23). This transcription factor is the homologue of *Bacillus* species MntR which is known to bind two Mn²⁺ ions as corepressors (15). The gene encoding the zinc efflux pump CzcD also showed increased expression under Mn²⁺-limited conditions in wild-type cells. The expression of *czcD* is known to be under the control of the transcriptional factor SczA that activates expression in response to elevated Zn²⁺ levels (22, 53). Thus, a decrease in intracellular Mn²⁺ may be associated with an increase in intracellular Zn²⁺. It has been reported that Zn²⁺ binding to PsaR may antagonize its action as a repressor (20, 40). Thus, perturbation of the Mn²⁺/Zn²⁺ ratio caused by

Mn²⁺ limitation may cause altered gene expression in wild-type *S. pneumoniae*. A similar pattern of gene expression was observed in the A− versus A+ comparison. This demonstrates that PsaR is exerting its regulatory influence on gene expression in the mutant. The *czcD* gene was also induced but, in addition, the *nmlR* and *adhC* genes were also upregulated. *czcD-nmlR-adhC* form a gene cluster (spd1636-1638). Thus, it is possible that under conditions of severe Mn²⁺ limitation such as for the A− strain, there are changes in the transcription of this gene cluster and *nmlR* and *adhC* are expressed as part of a polycistronic transcript as a consequence of read-through from the *czcD* gene, or alternatively, as a distinct transcript from the *nmlR* promoter. In *Haemophilus influenzae*, *adhC* encodes a glutathione-dependent alcohol dehydrogenase that is required for defense against oxidative and nitrosative stress (21). This suggests that under conditions of Mn²⁺ limitation, a glutathione-based defense system could manifest itself in the pneumococcus. The gene expression changes may relate to the different niches in which *S. pneumoniae* is located within the human host; the nasopharynx is known to contain high levels of Mn²⁺ (36 μM quoted for saliva) (6), while in blood serum, it is about 20 nM (18, 26, 48). The relative concentrations of total glutathione in the nasopharynx and whole blood are <0.5 μM and 11 μM, respectively (41, 42). Interestingly, we have previously observed that *adhC* and *nmlR* mutants show reduced survival in blood compared to the survival of wild-type cells in a murine infection model, although the strains exhibited similar survival in the nasopharynx (22, 53). This would be consistent with a switch from a Mn²⁺-based to a glutathione-based stress defense system. A model for the central role of Mn²⁺ in this process is proposed in Fig. 5.

S. pneumoniae is not thought to synthesize glutathione (14), indicating that it would need to acquire this tripeptide. This could be a function of the *appDCBA* operon that encodes a polyspecific oligopeptide ABC transporter. The relative increase in the mRNA abundance of the *appDCBA* operon coincides with a decrease in the level of the PepA protein (spd1647). *In silico* analysis indicated that PepA had structural
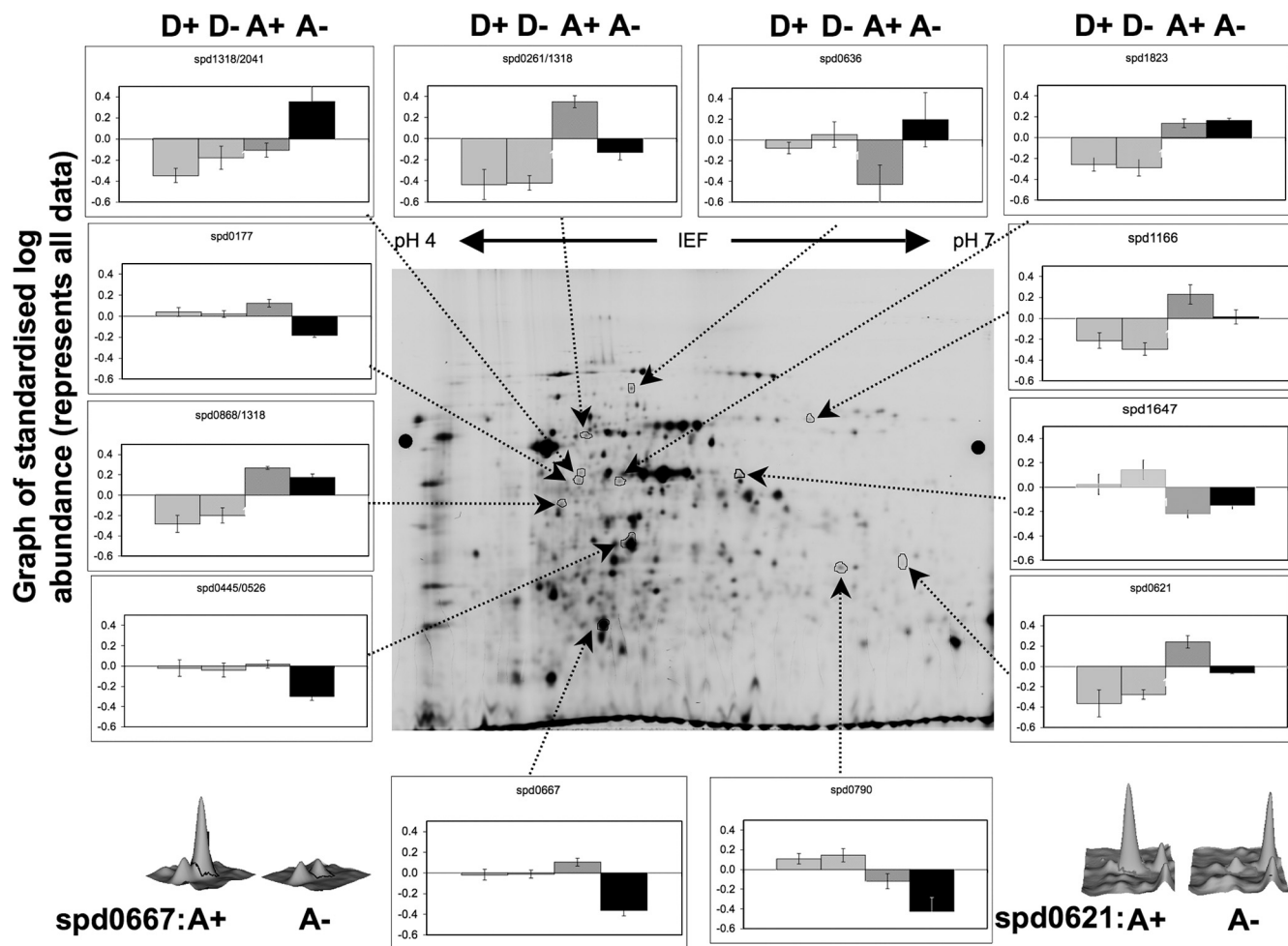
FIG. 4. DIGE analysis of protein spots from *S. pneumoniae* D39 wild type and its isogenic *psaA* deletion mutant. Graphs of standardized log abundances of 12 highly regulated spots and three-dimensional images of standardized log abundances of the Mn^{2+}-dependent superoxide dismutase (SodA; spd0667) and lactate oxidase (LctO; spd0621) are shown. D+, D39 wild type grown in C+Y+M medium; D−, D39 wild type grown in C+Y medium; A+, D39 *psaA* deletion mutant grown in C+Y+M medium; A−, D39 *psaA* deletion mutant grown in C+Y medium.

motifs of a tripeptidase, an enzyme that has been shown to cleave reduced glutathione (GSH) to generate cysteine (8), which is critical for intracellular growth (1). Thus, downregulation in the *psaA* mutant would suggest that hydrolysis of GSH

TABLE 3. Intracellular metal ion concentrations of *S. pneumoniae* D39 wild type and its isogenic *psaA* deletion mutant counterpart grown in C+Y medium with and without 3 μM added Mn^{2+}

Strain[b]	Concn (ng/g cells) of[a]:	
	Mn^{2+}	Zn^{2+}
A−	89.81 ± 1.6	6874.16 ± 44.0
A+	290.99 ± 7.1	6413.56 ± 116.2
D−	241.44 ± 10.3	12865.84 ± 1684.1
D+	1017.69 ± 60.3	12702.48 ± 3697.3

[a] Cells were grown to an A_{600} of 0.3, and metal ion values are the means ± standard errors of the means of the results for duplicate samples from two independent experiments.

[b] A+, D39 *psaA* deletion mutant grown in C+Y medium with 3 μM added Mn^{2+}; A−, D39 *psaA* deletion mutant grown in C+Y medium without added Mn^{2+}; D+, D39 wild type grown in C+Y medium with 3 μM added Mn^{2+}; D−, D39 wild type grown in C+Y medium without added Mn^{2+}.

would be lower in order to preserve the GSH pool that is necessary for management of the oxidative-stress response. LctO also showed an increase in expression in the comparison of A+ and D−. This enzyme catalyzes the oxidation of lactate and generates pyruvate and H_2O_2 (54). Conditions where lactate would be available to the pneumococcus as a carbon source would be in blood and in the neutrophil. In contrast, in the nasopharynx, it would be expected that the organism would produce lactate as a fermentation end product. Under these conditions, pyruvate can also be oxidized by SpxB to generate acetyl phosphate and H_2O_2 (54). The increased expression of SpxB in the A−/A+ cells suggests that there may be some posttranslational effects of Mn^{2+} on SpxB.

The utilization of a glutathione-based defense system by *S. pneumoniae* would require a mechanism for regeneration of the intracellular glutathione pool. Glutathione reductase serves to reduce both oxidized and environmentally acquired glutathione (glutathione disulfide [GSSG]). However, a consequence of this mechanism is the rapid depletion of intracellular NADPH levels (10). Concomitant with the deple-

FIG. 5. Diagrammatic representation of the proposed carbon metabolism in *psaA* mutants. The diagram shows the proposed flux of carbon in the *psaA* mutant strain as indicated by our biochemical, microarray, and proteomic data in D− and A+ cells. Wild-type cells utilized MnSOD to provide oxidative stress management, while the *psaA* mutant strains employed glutathione-based defense. Upregulated genes are indicated in red, and downregulated genes in blue. Abbreviations: G6P, glucose-6-phosphate; GAP, glyceradehyde-3-phosphate; PGK, phosphoglycerate kinase; PK, pyruvate kinase; Ldh, lactate dehydrogenase; Acetyl-P, acetyl phosphate; ROS, reactive oxygen species; G6PD, glucose-6-phosphate dehydrogenase; R5P, ribulose-5-phosphate; GSX, environmental glutathione; GSSH, oxidized glutathione; GSH, reduced glutathione.

tion of NADPH is the derepression of the pentose phosphate pathway (PPP) and diversion of carbon flux away from Embden-Meyerhoff metabolism. Consistent with this observation was the detection of the activity of the PPP enzyme, 6-phosphogluconate dehydrogenase (6-PGD), in both A+ and A− cells. This indicated that metabolic flux was being directed to the PPP in the *psaA* mutants, thus generating NADPH, consistent with the switch to a glutathione-based defense system under Mn^{2+} restriction.

In addition to these global changes to carbon metabolism, numerous minor alterations to cellular metabolism were also observed in response to Mn^{2+} concentrations. Notably, certain key enzymes involved in pyruvate metabolism, while not requiring Mn^{2+} for their function, exhibit their highest activity with Mn^{2+} as a cofactor (20). As a consequence, it would be expected that pyruvate precursor pools would be small, leading to increased flux through the glycolytic pathway and the upregulation of key enzymes. Under Mn^{2+}-replete conditions, oxidative stress would be ameliorated as Mn^{2+} could act directly to detoxify superoxide and H$_2$O$_2$ generated during metabolism (18). Although *S. pneumoniae* lacks catalase, it may be less sensitive to H$_2$O$_2$ than many bacteria because it contains only a small number of iron-containing proteins that could drive Fenton chemistry in the presence of H$_2$O$_2$. Recently, it has been suggested that Mn^{2+} can confer protection against peroxide stress on *Escherichia coli* by inserting into mononuclear metalloenzymes in place of ferrous iron (2). If Mn^{2+} is used predominantly in equivalent enzymes in *S. pneumoniae*, this would explain why the effect of upregulation of SpxB can be tolerated in Mn^{2+}-replete cells.

Colonization of the lungs is a key stage in the conversion of a local pneumococcal infection from the nasopharynx to a systemic infection. This is linked to the activation of alveolar macrophages and a subsequent heavy recruitment of neutrophils (24). A key pneumococcal virulence factor, pneumolysin, has been shown to activate the production of nitric oxide (NO) in neutrophils (17). Interestingly, NO is known to trigger the

release of Zn^{2+} from metallothionein as a response to lung injury (52). Thus, we suggest that a coupling of the expression of a glutathione-based oxidative- and nitrosative-stress defense system and the removal of excess Zn^{2+} may be linked to colonization of the lower respiratory tract.

Beyond the central role of Mn^{2+} in metabolic and oxidative-stress processes, putative roles in the regulation and activation of other proteins were also elucidated. In the proteomic analysis, EF-Tu and EF-Ts were upregulated in A− cells. EF-Ts is essential for the elongation of the polypeptide chain and mediates the regeneration of EF-Tu · GDP into the active form, EF-Tu · GTP, which transports aminoacyl-tRNA to the ribosome in the elongation cycle of protein synthesis (25, 39). We hypothesize that upregulation of the EF-Tu/EF-Ts in cells starved of Mn^{2+} might be necessary for protein stability. Genes encoding the heat shock proteins GroEL/GroES (spd1711) were downregulated in A− cells, most probably due to the lack of Mn^{2+} to stabilize GroEL under conditions of oxidative stress (36). Moreover, a peptidase M24 family protein (spd0177), a Mn^{2+}-dependent Xaa-Pro aminopeptidase (44), was upregulated in A+ cells, indicating the importance of Mn^{2+} as a cofactor in the activity of this enzyme.

Apart from the fundamental alterations to cellular metabolism and oxidative stress management, our transcriptome analyses have provided the first direct evidence for the essential role of PsaA in the induction of competence. Exogenous Mn^{2+} has long been implicated as a requirement for the development of competence for the genetic transformation of *psaA* mutants (9, 33, 34). In A− cells, downregulation of the transcriptional regulator ComX1 (spd0014), the competence-stimulating peptide (CSP; spd2065), and the competence operon (spd1857-1863) would be consistent with previous phenotypic observations (9, 33, 34).

In this study, gene expression and metabolic changes resulting from possible interaction between the genotypes of the strains (*psaA* mutation) and the growth conditions (with or without Mn^{2+}) regulating the expression of particular genes/

proteins were analyzed for synergy or interference. Microarray interaction analysis shows that a number of putative ABC transporters/transport systems (spd0097, spd0154, spd0616-0617, and spd1900) and a suite of genes involved in nucleotide metabolism (spd0187, spd0190, and spd1042) were downregulated in A− cells. However, a transcriptional regulator, a GntR family protein (spd1524), was highly upregulated in A− cells. Regulators belonging to this family have been shown to act as environmental sensors for controlling genes involved in responding directly or indirectly to external stimuli, such as small molecules or substrates (45). In addition, stress proteins (spd1590 and spd1793) were also upregulated in A− cells (see Table S3 in the supplemental material), probably due to oxidative stress. A further analysis to establish relationships in gene expression patterns due to *psaA* mutation and/or Mn^{2+} limitation was carried out using Venn diagrams (see Fig. S3 and Table S4 in the supplemental material). Protein interaction analysis highlighted those proteins whose regulation by the presence or absence of Mn^{2+} depended on the genotype. This is exemplified by the expression of EF-Tu/PepC and LctO, in which the genotypic effect is significantly suppressed under low Mn^{2+} conditions, and by the significant downregulation of the expression of PepM and SodA under low Mn^{2+} conditions in the *psaA* mutant (Table 2; also see Fig. S4 in the supplemental material).

Conclusions. In this study, we have used a combination of transcriptomic and/or proteomic approaches to provide evidence for Mn^{2+}-dependent regulation of the expression of the pneumococcal virulence-associated genes *pcpA* and *prtA* and the oxidative stress-response enzymes SpxB and Mn^{2+} SodA. Furthermore, the analyses provided direct evidence for high-affinity Mn^{2+} transport by PsaA in pneumococcal competence, physiology, and metabolism and elucidated the mechanisms underlying the response of the *psaA* mutant to Mn^{2+} stress. This serves as a paradigm for numerous mucosal pathogens which, like *S. pneumoniae*, are exposed to various levels of Mn^{2+} during disease pathogenesis, from asymptomatic nasopharyngeal colonization to the invasion of deeper host tissues.

REFERENCES

1. **Alkhuder, K., K. L. Meibom, I. Dubail, M. Dupuis, and A. Charbit.** 2009. Glutathione provides a source of cysteine essential for intracellular multiplication of *Francisella tularensis*. PLoS Pathog. **5:**e1000284.
2. **Anjem, A., S. Varghese, and J. A. Imlay.** 2009. Manganese import is a key element of the OxyR response to hydrogen peroxide in *Escherichia coli*. Mol. Microbiol. **72:**844–858.
3. **Avery, O. T., C. M. MacLeod, and M. McCarty.** 1944. Studies on the chemical nature of the substance inducing transformation of pneumococcal types. Inductions of transformation by a desoxyribonucleic acid fraction isolated from pneumococcus type III. J. Exp. Med. **79:**137–158.
4. **Berry, A. M., and J. C. Paton.** 1996. Sequence heterogeneity of PsaA, a 37-kilodalton putative adhesin essential for virulence of *Streptococcus pneumoniae*. Infect. Immun. **64:**5255–5262.
5. **Brown, A. T., and C. L. Wittenberger.** 1971. Mechanism for regulating the distribution of glucose carbon between the Embden-Meyerhof and hexose-monophosphate pathways in *Streptococcus faecalis*. J. Bacteriol. **106:**456–467.
6. **Chicharro, J. L., V. Serrano, R. Urena, A. M. Gutierrez, A. Carvajal, P. Fernandez-Hernando, and A. Lucia.** 1999. Trace elements and electrolytes in human resting mixed saliva after exercise. Br. J. Sports Med. **33:**204–207.
7. **Corbin, B. D., E. H. Seeley, A. Raab, J. Feldmann, M. R. Miller, V. J. Torres, K. L. Anderson, B. M. Dattilo, P. M. Dunman, R. Gerads, R. M. Caprioli, W. Nacken, W. J. Chazin, and E. P. Skaar.** 2008. Metal chelation and inhibition of bacterial growth in tissue abscesses. Science **319:**962–965.
8. **Del Corso, A., M. Cappiello, F. Buono, R. Moschini, A. Paolicchi, and U. Mura.** 2006. Colorimetric coupled enzyme assay for gamma-glutamyltransferase activity using glutathione as substrate. J. Biochem. Biophys. Methods **67:**123–130.
9. **Dintilhac, A., G. Alloing, C. Granadel, and J. P. Claverys.** 1997. Competence and virulence of *Streptococcus pneumoniae*: Adc and PsaA mutants exhibit a requirement for Zn and Mn resulting from inactivation of putative ABC metal permeases. Mol. Microbiol. **25:**727–739.
10. **Eggleston, L. V., and H. A. Krebs.** 1974. Regulation of the pentose phosphate cycle. Biochem. J. **138:**425–435.
11. **Eisen, M. B., P. T. Spellman, P. O. Brown, and D. Botstein.** 1998. Cluster analysis and display of genome-wide expression patterns. Proc. Natl. Acad. Sci. U. S. A. **95:**14863–14868.
12. **Encheva, V., S. E. Gharbia, R. Wait, S. Begum, and H. N. Shah.** 2006. Comparison of extraction procedures for proteome analysis of *Streptococcus pneumoniae* and a basic reference map. Proteomics **6:**3306–3317.
13. **Eriksson, L., E. Johansson, N. Kettaneh-Wold, and S. Wold.** 2001. Multi- and megavariate data analysis: principles and applications. Umetrics Academy, Umeå, Sweden.
14. **Fahey, R. C., W. C. Brown, W. B. Adams, and M. B. Worsham.** 1978. Occurrence of glutathione in bacteria. J. Bacteriol. **133:**1126–1129.
15. **Glasfeld, A., E. Guedon, J. D. Helmann, and R. G. Brennan.** 2003. Structure of the manganese-bound manganese transport regulator of *Bacillus subtilis*. Nat. Struct. Biol. **10:**652–657.
16. **Hendriksen, W. T., H. J. Bootsma, A. van Diepen, S. Estevao, O. P. Kuipers, R. de Groot, and P. W. Hermans.** 2009. Strain-specific impact of PsaR of *Streptococcus pneumoniae* on global gene expression and virulence. Microbiology **155:**1569–1579.
17. **Hirst, R. A., A. Kadioglu, C. O'Callaghan, and P. W. Andrew.** 2004. The role of pneumolysin in pneumococcal pneumonia and meningitis. Clin. Exp. Immunol. **138:**195–201.
18. **Johnston, J. W., D. E. Briles, L. E. Myers, and S. K. Hollingshead.** 2006. Mn^{2+}-dependent regulation of multiple genes in *Streptococcus pneumoniae* through PsaR and the resultant impact on virulence. Infect. Immun. **74:**1171–1180.
19. **Johnston, J. W., L. E. Myers, M. M. Ochs, W. H. Benjamin, Jr., D. E. Briles, and S. K. Hollingshead.** 2004. Lipoprotein PsaA in virulence of *Streptococcus pneumoniae*: surface accessibility and role in protection from superoxide. Infect. Immun. **72:**5858–5867.
20. **Kehres, D. G., and M. E. Maguire.** 2003. Emerging themes in manganese transport, biochemistry and pathogenesis in bacteria. FEMS Microbiol. Rev. **27:**263–290.
21. **Kidd, S. P., D. Jiang, M. P. Jennings, and A. G. McEwan.** 2007. Glutathione-dependent alcohol dehydrogenase AdhC is required for defense against nitrosative stress in *Haemophilus influenzae*. Infect. Immun. **75:**4506–4513.
22. **Kloosterman, T. G., M. M. van der Kooi-Pol, J. J. Bijlsma, and O. P. Kuipers.** 2007. The novel transcriptional regulator SczA mediates protection against Zn^{2+} stress by activation of the Zn^{2+}-resistance gene *czcD* in *Streptococcus pneumoniae*. Mol. Microbiol. **65:**1049–1063.
23. **Kloosterman, T. G., R. M. Witwicki, M. M. van der Kooi-Pol, J. J. Bijlsma, and O. P. Kuipers.** 2008. Opposite effects of Mn^{2+} and Zn^{2+} on PsaR-mediated expression of the virulence genes *pcpA*, *prtA*, and *psaBCA* of *Streptococcus pneumoniae*. J. Bacteriol. **190:**5382–5393.
24. **Knapp, S., J. C. Leemans, S. Florquin, J. Branger, N. A. Maris, J. Pater, N. van Rooijen, and T. van der Poll.** 2003. Alveolar macrophages have a protective antiinflammatory role during murine pneumococcal pneumonia. Am. J. Respir. Crit. Care Med. **167:**171–179.
25. **Krab, I. M., and A. Parmeggiani.** 1998. EF-Tu, a GTPase odyssey. Biochim. Biophys. Acta **1443:**1–22.
26. **Krachler, M., E. Rossipal, and D. Micetic-Turk.** 1999. Concentrations of trace elements in sera of newborns, young infants, and adults. Biol. Trace Elem. Res. **68:**121–135.
27. **Lacks, S., and R. D. Hotchkiss.** 1960. A study of the genetic material determining an enzyme in Pneumococcus. Biochim. Biophys. Acta **39:**508–518.
28. **Laemmli, U. K.** 1970. Cleavage of structural proteins during the assembly of the head of bacteriophage T4. Nature **227:**680–685.
29. **Lawrence, M. C., P. A. Pilling, V. C. Epa, A. M. Berry, A. D. Ogunniyi, and J. C. Paton.** 1998. The crystal structure of pneumococcal surface antigen PsaA reveals a metal-binding site and a novel structure for a putative ABC-type binding protein. Structure **6:**1553–1561.
30. **LeMessurier, K. S., A. D. Ogunniyi, and J. C. Paton.** 2006. Differential

expression of key pneumococcal virulence genes *in vivo*. Microbiology. **152:** 305–311.

31. **Livak, K. J., and T. D. Schmittgen.** 2001. Analysis of relative gene expression data using real-time quantitative PCR and the $2^{-\Delta\Delta CT}$ Method. Methods **25:**402–408.

32. **Loisel, E., L. Jacquamet, L. Serre, C. Bauvois, J. L. Ferrer, T. Vernet, A. M. Di Guilmi, and C. Durmort.** 2008. AdcAII, a new pneumococcal Zn-binding protein homologous with ABC transporters: biochemical and structural analysis. J. Mol. Biol. **381:**594–606.

33. **Marra, A., S. Lawson, J. S. Asundi, D. Brigham, and A. E. Hromockyj.** 2002. *In vivo* characterization of the *psa* genes from *Streptococcus pneumoniae* in multiple models of infection. Microbiology. **148:**1483–1491.

34. **McAllister, L. J., H. J. Tseng, A. D. Ogunniyi, M. P. Jennings, A. G. Mc-Ewan, and J. C. Paton.** 2004. Molecular analysis of the *psa* permease complex of *Streptococcus pneumoniae*. Mol. Microbiol. **53:**889–901.

35. **McCluskey, J., J. Hinds, S. Husain, A. Witney, and T. J. Mitchell.** 2004. A two-component system that controls the expression of pneumococcal surface antigen A (PsaA) and regulates virulence and resistance to oxidative stress in *Streptococcus pneumoniae*. Mol. Microbiol. **51:**1661–1675.

36. **Melkani, G. C., R. L. Sielaff, G. Zardeneta, and J. A. Mendoza.** 2008. Divalent cations stabilize GroEL under conditions of oxidative stress. Biochem. Biophys. Res. Commun. **368:**625–630.

37. **Novak, R., J. S. Braun, E. Charpentier, and E. Tuomanen.** 1998. Penicillin tolerance genes of *Streptococcus pneumoniae*: the ABC-type manganese permease complex Psa. Mol. Microbiol. **29:**1285–1296.

38. **Ogunniyi, A. D., P. Giammarinaro, and J. C. Paton.** 2002. The genes encoding virulence-associated proteins and the capsule of *Streptococcus pneumoniae* are upregulated and differentially expressed *in vivo*. Microbiology **148:**2045–2053.

39. **Overweg, K., C. D. Pericone, G. G. Verhoef, J. N. Weiser, H. D. Meiring, A. P. De Jong, R. De Groot, and P. W. Hermans.** 2000. Differential protein expression in phenotypic variants of *Streptococcus pneumoniae*. Infect. Immun. **68:**4604–4610.

40. **Papp-Wallace, K. M., and M. E. Maguire.** 2006. Manganese transport and the role of manganese in virulence. Annu. Rev. Microbiol. **60:**187–209.

41. **Pastore, A., R. Massoud, C. Motti, A. Lo Russo, G. Fucci, C. Cortese, and G. Federici.** 1998. Fully automated assay for total homocysteine, cysteine, cysteinylglycine, glutathione, cysteamine, and 2-mercaptopropionylglycine in plasma and urine. Clin. Chem. **44:**825–832.

42. **Pastore, A., F. Piemonte, M. Locatelli, A. Lo Russo, L. M. Gaeta, G. Tozzi, and G. Federici.** 2001. Determination of blood total, reduced, and oxidized glutathione in pediatric subjects. Clin. Chem. **47:**1467–1469.

43. **Paton, J. C.** 1998. Novel pneumococcal surface proteins: role in virulence and vaccine potential. Trends Microbiol. **6:**85–87. (Discussion, **6:**87–88.)

44. **Rawlings, N. D., and A. J. Barrett.** 1993. Evolutionary families of peptidases. Biochem. J. **290**(Pt. 1)**:**205–218.

45. **Rigali, S., A. Derouaux, F. Giannotta, and J. Dusart.** 2002. Subdivision of the helix-turn-helix GntR family of bacterial regulators in the FadR, HutC, MocR, and YtrA subfamilies. J. Biol. Chem. **277:**12507–12515.

46. **Rogers, T. J., A. W. Paton, S. R. McColl, and J. C. Paton.** 2003. Enhanced CXC chemokine responses of human colonic epithelial cells to locus of enterocyte effacement-negative shiga-toxigenic *Escherichia coli*. Infect. Immun. **71:**5623–5632.

47. **Russell, H., J. A. Tharpe, D. E. Wells, E. H. White, and J. E. Johnson.** 1990. Monoclonal antibody recognizing a species-specific protein from *Streptococcus pneumoniae*. J. Clin. Microbiol. **28:**2191–2195.

48. **Scheuhammer, A. M., and M. G. Cherian.** 1985. Binding of manganese in human and rat plasma. Biochim. Biophys. Acta **840:**163–169.

49. **Smyth, G. K.** 2005. Limma: linear models for microarray data, p. 397–420. *In* V. Carey, R. Gentleman, S. Dudoit, R. Irizarry, and W. Huber (ed.), Bioinformatics and computational biology solutions using R and Bioconductor. Springer, New York, NY.

50. **Smyth, G. K.** 2004. Linear models and empirical Bayes methods for assessing differential expression in microarray experiments. Stat. Appl. Genet. Mol. Biol. **3:**Article3.

51. **Smyth, G. K., and T. Speed.** 2003. Normalization of cDNA microarray data. Methods **31:**265–273.

52. **St. Croix, C. M., K. Leelavaninchkul, S. C. Watkins, V. E. Kagan, and B. R. Pitt.** 2005. Nitric oxide and zinc homeostasis in acute lung injury. Proc. Am. Thorac. Soc. **2:**236–242.

53. **Stroeher, U. H., S. P. Kidd, S. L. Stafford, M. P. Jennings, J. C. Paton, and A. G. McEwan.** 2007. A pneumococcal MerR-like regulator and S-nitrosoglutathione reductase are required for systemic virulence. J. Infect. Dis. **196:**1820–1826.

54. **Taniai, H., K. Iida, M. Seki, M. Saito, S. Shiota, H. Nakayama, and S. Yoshida.** 2008. Concerted action of lactate oxidase and pyruvate oxidase in aerobic growth of *Streptococcus pneumoniae*: role of lactate as an energy source. J. Bacteriol. **190:**3572–3579.

55. **Tettelin, H., K. E. Nelson, I. T. Paulsen, J. A. Eisen, T. D. Read, S. Peterson, J. Heidelberg, R. T. DeBoy, D. H. Haft, R. J. Dodson, A. S. Durkin, M. Gwinn, J. F. Kolonay, W. C. Nelson, J. D. Peterson, L. A. Umayam, O. White, S. L. Salzberg, M. R. Lewis, D. Radune, E. Holtzapple, H. Khouri, A. M. Wolf, T. R. Utterback, C. L. Hansen, L. A. McDonald, T. V. Feldblyum, S. Angiuoli, T. Dickinson, E. K. Hickey, I. E. Holt, B. J. Loftus, F. Yang, H. O. Smith, J. C. Venter, B. A. Dougherty, D. A. Morrison, S. K. Hollingshead, and C. M. Fraser.** 2001. Complete genome sequence of a virulent isolate of *Streptococcus pneumoniae*. Science **293:**498–506.

56. **Towbin, H., T. Staehelin, and J. Gordon.** 1979. Electrophoretic transfer of proteins from polyacrylamide gels to nitrocellulose sheets: procedure and some applications. Proc. Natl. Acad. Sci. U. S. A. **76:**4350–4354.

57. **Tseng, H. J., A. G. McEwan, J. C. Paton, and M. P. Jennings.** 2002. Virulence of *Streptococcus pneumoniae*: PsaA mutants are hypersensitive to oxidative stress. Infect. Immun. **70:**1635–1639.

58. **Yesilkaya, H., A. Kadioglu, N. Gingles, J. E. Alexander, T. J. Mitchell, and P. W. Andrew.** 2000. Role of manganese-containing superoxide dismutase in oxidative stress and virulence of *Streptococcus pneumoniae*. Infect. Immun. **68:**2819–2826.